Published OnlineFirst September 15, 2010; DOI: 10.1158/1078-0432.CCR-09-3293

Clinical Cancer Research

A Proteasome Inhibitor, Bortezomib, Inhibits Breast Cancer Growth and Reduces Osteolysis by Downregulating Metastatic Genes

Marci D. Jones, Julie C. Liu, Thomas K. Barthel, et al.

Clin Cancer Res 2010;16:4978-4989. Published OnlineFirst September 15, 2010.

Published OnlineFirst September 15, 2010; DOI: 10.1158/1078-0432.CCR-09-3293

Cancer Therapy: Preclinical

Clinical Cancer Research

A Proteasome Inhibitor, Bortezomib, Inhibits Breast Cancer Growth and Reduces Osteolysis by Downregulating Metastatic Genes

Marci D. Jones[1,2], Julie C. Liu[1], Thomas K. Barthel[2], Sadiq Hussain[1], Erik Lovria[2], Dengfeng Cheng[3], Jesse A. Schoonmaker[5], Sudhanshu Mulay[5], David C. Ayers[2], Mary L. Bouxsein[4], Gary S. Stein[1], Siddhartha Mukherjee[5,6], and Jane B. Lian[1]

Abstract

Purpose: The incidence of bone metastasis in advanced breast cancer (BrCa) exceeds 70%. Bortezomib, a proteasome inhibitor used for the treatment of multiple myeloma, also promotes bone formation. We tested the hypothesis that proteasome inhibitors can ameliorate BrCa osteolytic disease.

Experimental Design: To address the potentially beneficial effect of bortezomib in reducing tumor growth in the skeleton and counteracting bone osteolysis, human MDA-MB-231 BrCa cells were injected into the tibia of mice to model bone tumor growth for *in vivo* assessment of treatment regimens before and after tumor growth.

Results: Controls exhibited tumor growth, destroying trabecular and cortical bone and invading muscle. Bortezomib treatment initiated following inoculation of tumor cells strikingly reduced tumor growth, restricted tumor cells mainly to the marrow cavity, and almost completely inhibited osteolysis in the bone microenvironment over a 3- to 4-week period as shown by [^{18}F]fluorodeoxyglucose positron emission tomography, micro–computed tomography scanning, radiography, and histology. Thus, proteasome inhibition is effective in killing tumor cells within the bone. Pretreatment with bortezomib for 3 weeks before inoculation of tumor cells was also effective in reducing osteolysis. Our *in vitro* and *in vivo* studies indicate that mechanisms by which bortezomib inhibits tumor growth and reduces osteolysis result from inhibited cell proliferation, necrosis, and decreased expression of factors that promote BrCa tumor progression in bone.

Conclusion: These findings provide a basis for a novel strategy to treat patients with BrCa osteolytic lesions, and represent an approach for protecting the entire skeleton from metastatic bone disease. *Clin Cancer Res; 16(20); 4978–89. ©2010 AACR.*

Metastatic osteolytic disease is prevalent in cancer patients. In advanced breast cancer (BrCa), 70% of women develop osteolytic lesions, resulting in pain, pathologic fracture, and increased morbidity. Dysfunction of the ubiquitin-proteasome system is associated with tumor growth and metastatic disease, providing the rationale for development of proteasome inhibitors as antineoplastic therapies (1, 2). The proteasome is a ubiquitous enzyme complex that plays a critical role in the degradation of proteins involved in cell cycle regulation, apoptosis, and angiogenesis (2, 3). Bortezomib, a selective proteasome inhibitor used to treat multiple myeloma, has a potent anabolic effect on bone (4–9). Bortezomib alters the bone marrow microenvironment by increasing the number and differentiation of resident mesenchymal stem cells into osteoblasts, thereby increasing bone formation rates within 4 weeks in normal mice and resulting in trabecular bone formation in bone loss model (7). A similar enhancement of osteoblast differentiation is found in myeloma patients treated with bortezomib who show sustained increases in circulating osteocalcin, a marker of bone formation (6, 10). Thus, bortezomib treatment represents a novel and clinically feasible approach for increasing bone formation in the setting of the osteolytic bone disease accompanying metastatic breast, prostate, and lung cancers (4, 5, 11).

Nonsurgical treatment of bone metastatic lesions includes radiation therapy and bisphosphonates. Bisphosphonates were initially reported to reduce the risk of

Authors' Affiliations: [1]Department of Cell Biology and Cancer Center, [2]Department of Orthopedics and Physical Rehabilitation, and [3]Division of Nuclear Medicine, Department of Radiology, University of Massachusetts Medical School, Worcester, Massachusetts; [4]Center for Advanced Orthopedic Studies, Beth Israel Deaconess Medical Center; [5]Center for Regenerative Medicine, Massachusetts General Hospital, Boston, Massachusetts; and [6]Herbert Irving Comprehensive Cancer Center, Columbia University, New York, New York

Note: Current address for J.C. Liu is School of Chemical Engineering, Purdue University, West Lafayette, Indiana.

Corresponding Author: Jane B. Lian, Department of Cell Biology, University of Massachusetts Medical School, 55 Lake Avenue North, Worcester, MA 01655. Phone: 508-856-5625; Fax: 508-856-6800; E-mail: jane.lian@umassmed.edu.

doi: 10.1158/1078-0432.CCR-09-3293

Published OnlineFirst September 15, 2010; DOI: 10.1158/1078-0432.CCR-09-3293

Translational Relevance

Breast cancer (BrCa) metastasis to the bone and osteolytic lesions typically caused by these metastases are particularly resistant to pharmacologic therapy. This study shows that the Food and Drug Administration–approved proteasome inhibitor bortezomib strikingly decreases the size of BrCa metastatic tumors and associated osteolytic lesions through multiple mechanisms: by inducing cellular necrosis and apoptosis, inhibiting tumor cell Wnt signaling and matrix degradation, and reducing vascularization. In addition, the proteosome inhibitor provided a significant skeleton-wide bone anabolic effect, despite the presence of a metastatic lesion. Current treatment of metastases with bisphosphonates limits bone resorption but does not rebuild bone volume lost to osteolysis. Our findings also provide evidence for increased capability to treat BrCa osteolytic disease preemptively using bortezomib before tumor cell growth in bone by inhibiting tumor responses to the bone microenvironment and by providing protective anabolic effects on the skeleton.

pathologic fracture and bone pain, although a recent study totaling over 7,000 BrCa patients indicated no reduction in fracture risk compared with placebo or no treatment groups (12–14). In addition, bisphosphonates at doses required for cancer patients can have a significant side effect profile (15, 16), and alternate approaches to protect the skeleton are needed.

Tumor cells in the bone microenvironment overcome the marrow compartment and inhibit the ability of sufficient stromal cells to differentiate into osteoblasts to replace lost bone. Cancer cells secrete factors that induce a vicious cycle of osteoclast activation and growth factor release that promotes tumor survival. Bortezomib contributes to the apoptosis of tumor cells and tumor-activated osteoclasts (17–19); as well, low-dose bortezomib promotes bone anabolic effects in mice (7). Given the aggressive osteolytic disease produced by BrCa cells that metastasize to the bone, we investigated the effectiveness of bortezomib treatment for inhibiting rapid tumor growth within the bone, and the potential for retaining bone volume. We postulated that bortezomib treatment could be an effective therapy by suppressing growth of the metastatic tumor (4, 7–9, 20–22), inhibiting osteoclastogenesis and survival (9, 17, 21, 23–26), and stabilizing osteoprogenitor cells within the marrow (26), or by a combination of all these effects.

Materials and Methods

Cell culture

The metastatic human BrCa MDA-MB-231 (American Type Culture Collection HTB-22) and mouse preosteoblast MC3T3-E1 (American Type Culture Collection CRL-2593) cell lines were used. Cells were cultured in α-MEM containing 10% fetal bovine serum (Invitrogen, Inc.). Cells were maintained at 37°C in a humidified incubator with 5% CO_2.

Animal care

Approval from the Institutional Animal Care and Use Committee was obtained. Six-week-old female severe combined immunodeficient (NCr/SCID) mice were housed in pathogen-free conditions and used for all experiments. Per experiment, groups contained three mice, and all studies except for the bortezomib pretreatment and continuous bortezomib experiment comparison (Fig. 4) were repeated for a total of six to eight mice per group. The repeat studies were terminated at either 6 or 7 weeks. At sacrifice, all mice were analyzed radiographically at weekly intervals followed by either histology, micro–computed tomography (μCT), or positron emission tomography (PET)/single-photon emission CT (SPECT) imaging at sacrifice.

Tibial implantation of MDA-MB-231 cells and bortezomib treatment

Mice were anesthetized with 0.15 mg ketamine/0.015 mg xylazine i.p. per gram of body weight. A medial parapatellar incision was created, and a needle was placed in the intramedullary canal of the tibia by aid of fluoroscopy (XiScan 1000-1, XiTec). MDA-MB-231 cells (1×10^5 in 100 μL of PBS) were slowly injected into the tibia and closed with 5-0 chromic suture (Ethicon, Inc.). Mice were given 0.1 mg/kg buprenorphine subcutaneous (SQ) postoperatively. Bortezomib (Millennium Pharmaceuticals) i.p. injections at a dose of 0.3 mg/kg body weight were begun 24 hours after intratibial injection and continued three times a week, or as indicated in each study.

Histologic analysis

Following sacrifice, the lower extremities were dissected and then fixed in 4% paraformaldehyde and decalcified in 18% EDTA (pH 8.0). Paraffin sections were cut at 6-μm thickness and stained with routine H&E, TRAP, or Ki-67 immunohistochemistry (27). Photomicrographs were acquired on a Zeiss Axioskop 40 microscope with attached AxioCam HRC and analyzed by AxioVision Rel 4.7 software (Carl Zeiss MicroImaging).

Radiographic analysis

Osteolysis was monitored by serial radiographs using a Faxitron MX-20 X-ray machine unit. We devised a scale to measure the severity of osteolytic lesions based on their appearance by conventional radiography. Blinded radiographs were evaluated by seven different scorers, and significant differences were determined by Student's t test. Osteolytic lesions were scored on a scale of 0 to 5 based on their severity: 0, no visible osteolysis; 5, most severe degree of osteolysis. A grade 1 lesion was small, isolated, and <10% of the width of the bone; grade 2 included single or multifocal small lesions, <33% of the cortical

Published OnlineFirst September 15, 2010; DOI: 10.1158/1078-0432.CCR-09-3293

width; grade 3 lesions have a size of 33% to 75% of the cortical width; extensive lesions with >75% of the cortical width are graded as 4; and pathologic fracture with extensive cortical destruction represents a grade 5 lesion.

μCT analysis

Specimens were scanned using a high-resolution desktop microtomographic imaging system (μCT40, Scanco Medical AG) using an isotropic voxel size of 12 μm, as previously described (28–30). In tumored bone, total bone volume is assessed by μCT by selecting the region of each tibia from the knee joint to the most proximal aspect of the proximal tibial-fibular joint, which ranges from 575 to 650 sections. In the nontumored distal femur, bone was evaluated in the region starting 360 μm proximal to the growth plate and extending 1,800 μm proximally. For bone regions without tumors, we assessed the trabecular bone volume fraction (%), trabecular thickness (μm), trabecular number (mm^{-1}), trabecular separation (μm), connectivity density ($1/mm^3$), and structure model index (SMI). Results were analyzed for significant differences by Student's *t* test.

PET/CT animal imaging

Bioscan NanoSPECT/CT and Philips Mosaic HP PET cameras were used to collect CT and [^{18}F]fluorodeoxyglucose (FDG) images of mice. Tumored mice were anesthetized and injected i.v. with 100 μCi of ^{18}F-FDG, and PET imaging was done at 30 minutes after administration. All data imaging and analysis were done at the University of Massachusetts Small Animal Imaging Core Facility. After each PET acquisition, the mouse, immobilized on the Minerva bed (Bioscan), was transferred to NanoSPECT/CT camera for the CT acquisition. The CT acquisition was done at standard frame resolution, 45 kVp tube voltage, and 500 ms of exposure time. The CT reconstruction was done using InVivoScope 1.37 software (Bioscan), and a PET/CT fusion image was created.

Real-time reverse transcription-PCR analysis

mRNA levels of metastatic and osteolytic-related genes were analyzed from MDA-MB-231 cells, MC3T3 cells, or BrCa tumor following bortezomib treatment. RNA was isolated using Trizol (Invitrogen) according to the manufacturer's protocol. Oligo(dT) primers were used in conjunction with the SuperScript First-Strand Synthesis System (Invitrogen) to synthesize cDNAs. Primer sequences are as follows: mouse: alkaline phosphatase (AP), TTGTGCGAGAGAAAGAGAGAGA (forward) and GTTTCAGGGCATTTTTCAAGGT (reverse); collagen type 1A (COL1A), CCCAAGGAAAAGAAGCACGTC (forward) and AGGTCAGCTGGATAGCGACATC (reverse); DKK3, TGCACCAGGAAGTTCACAAG (forward) and GGCCCACAGTCTTCATCAAT (reverse); glyceraldehyde-3-phosphate dehydrogenase (GAPDH), AGGTCGGTGTGAACGGATTTG (forward) and TGTAGACCATGTAGTTGAGGTCA (reverse); lymphoid enhanced binding factor 1 (LEF1), AGTGCAGCTATCAACCAGAT (forward) and TTCATAGTATTTGGCCTGCT (reverse); RUNX2, CGGCCCTCCCTGAACTCT (forward) and TGCCTGCCTGGGATCTGTA (reverse); transcription factor 4 (TCF4), CAGAATCCACAGATACAGCA (forward) and CAGCCTTTGAAATCTTCATC (reverse); human: Dickkopf 1 (DKK1), TCATTTCCGAGGAGAAATTGAG (forward) and AACCTTCTTGTCCTTTGGTG (reverse); GAPDH, ATGTTCGTCATGGGTGTGAA (forward) and TGTGGTCATGAGTCCTTCCA (reverse); LEF1, CCCGAGAACATCAAATAAAGTG (forward) and CTCTACAACAAGGGACCCTC (reverse); matrix metalloproteinase-9 (MMP-9), CCTGGAGACCTGAGAACCAATC (forward) and CCACCCGAGTGTAACCATAGC (reverse); receptor activator for NF-κB ligand (RANKL), CACATCAGAGCAGAGAAAGC (forward) and CTTTATGGGAACCAGATGGG (reverse); RUNX2, CGGCCCTCCCTGAACTCT (forward) and TGCCTGCCTGGGGTCTGTA (reverse); and vascular endothelial growth factor (VEGF), TCTTCAAGCCATCCTGTGTG (forward) and GCGAGTCTGTGTTTTTGCAG (reverse). Real-time PCR analysis was done to confirm expression levels by using an ABI machine and PRISM software (Applied Biosystems); significant differences were determined by Student's *t* test.

Annexin V binding and fluorescence-activated cell sorting analysis

Bortezomib-treated MDA-MB-231 cells were stained with Annexin V–FITC and propidium iodide (PI) using the Annexin V–FITC Apoptosis Detection kit (BD Biosciences). Stained live cells were submitted to the Flow Cytometry Core Lab at the University of Massachusetts for fluorescence-activated cell sorting (FACS) analysis (FACSCalibur, BD Biosciences). All fluorescent parameters were acquired in logarithmic amplification, and forward and side scatter parameters were acquired in linear. Data were analyzed using CellQuest software.

Results

Bortezomib slows the growth of osteolytic lesions caused by BrCa tumors in the bone microenvironment

Given the anabolic effects of bortezomib on bone in multiple myeloma, we investigated if bortezomib treatment could ameliorate the osteolysis caused by BrCa cells in bone. Mice that received intratibial inoculations of MDA-MB-231 BrCa cells were treated with 0.3 mg/kg body weight bortezomib administered three times a week for 7 weeks. This dose and schedule represents the highest bortezomib dose used in a study in which the serum osteocalcin level, a marker of bone formation, was found to increase in response to bortezomib treatment (7). We observed this dose to be nontoxic throughout the duration of the study ($n > 24$ mice).

Radiographs in Fig. 1A (three representative tibias) show osteolytic lesions in controls at day 21 that are inhibited by bortezomib treatment. By 35 days, small focal areas of missing trabeculae were observed with bortezomib treatment. With continued bortezomib (to day 49 in

Published OnlineFirst September 15, 2010; DOI: 10.1158/1078-0432.CCR-09-3293

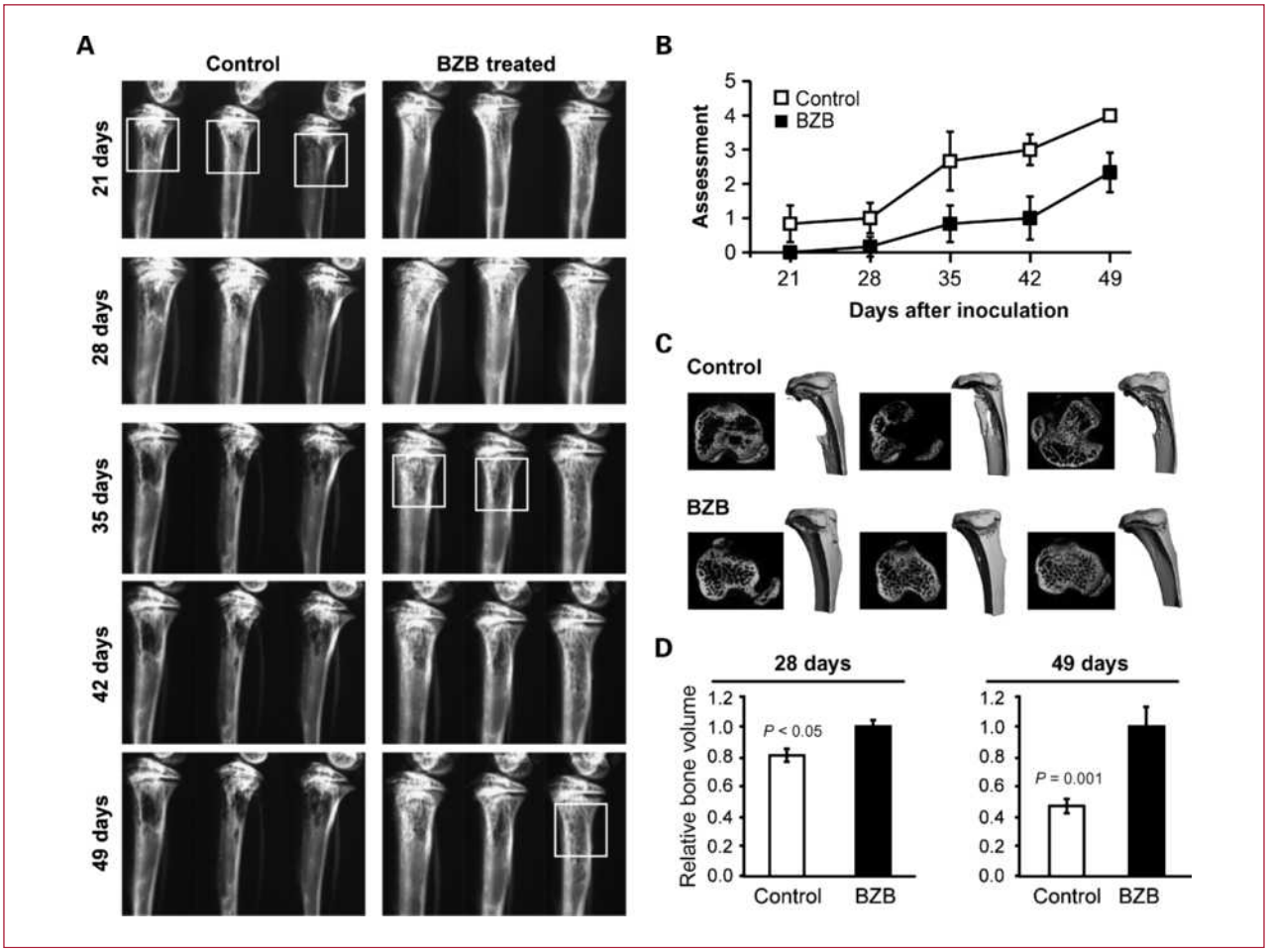

Fig. 1. Bortezomib slows growth of BrCa osteolytic lesions as seen by conventional radiographs and μCT. A, radiographs of NCr/SCID mice during progression of tumor growth. Mice ($n = 3$) received intratibial injection of 100,000 MDA-MB-231 BrCa cells and were treated with bortezomib (BZB) or PBS (0.3 mg/kg i.p.; three times per week) until sacrifice at 49 d following BrCa injection. Interval radiographs are shown, indicating a delay in the onset of osteolysis in bortezomib-treated mice. There is an absence of clearly defined lesions in bortezomib-treated mice until day 35; in contrast, the control group has clear osteolysis by day 21 (box). Microlytic lesions are seen in the bortezomib group on day 35 (box). B, quantitation of radiographs. Average score (see Materials and Methods) from each time point and all reviewers for control and bortezomib-treated mice is presented. This shows the presence of osteolysis from day 21 in control-treated mice but delay of osteolysis until day 35 in the bortezomib-treated group. Additionally, the increase in osteolysis during the final week of the experiment (days 42-49) is shown (days 21 and 28, $P < 0.05$; days 35, 42, and 49, $P < 0.005$). C, μCT images. Transverse section distal to the physis (left) and three-dimensional reconstruction of the proximal tibia (right) of bortezomib- and control-treated mice ($n = 3$) 49 d following intratibial injection of MDA-MB-231 BrCa cells. The reduction in osteolysis is evident by an unresorbed periosteal surface in bortezomib-treated compared with control group. D, quantitation of μCT images. Relative bone volume at time was assessed by μCT analysis of the proximal tibia in two separate experiments at 28 d ($n = 5$) and 49 d ($n = 3$). The relative bone volume was significantly lower in control-treated compared with bortezomib-treated mice ($P < 0.05$, 28 d; $P = 0.001$, 49 d).

Fig. 1A), there was evidence of a slow rate of progression of bone lysis in the majority (~70%) of the bortezomib-treated mice in multiple independent experiments. At termination of studies, control mice had very large tumors causing significant morbidity, whereas the bortezomib groups consistently had greatly reduced bone loss in the region of the tumor cell inoculation when compared with control-treated mice. These conclusions are in part based on a semiquantitative evaluation of the radiographs based on a scoring system (see Materials and Methods; Fig. 1B). An aggressive increase in osteolysis was observed in controls after day 28 when tumor destroyed the cortical bone, invaded the surrounding tissue, and contributed to osteolysis from the periosteal side of bone as well as from the medullary cavity. In the bortezomib group, a clear inhibition of osteolytic disease is delayed until 4 to 5 weeks. After this point, low levels of osteolytic activity occurred, indicated by the appearance of lesions at the end of the study (Fig. 1A). A similar late appearance of osteolytic lesions was observed in different experiments (data not shown).

The tumor-containing tibias were further analyzed by *ex vivo* μCT in three mice. Figure 1C shows tibias of control mice with extensive osteolytic disease eroding through the cortex, whereas the tibias of the bortezomib-treated mice

Published OnlineFirst September 15, 2010; DOI: 10.1158/1078-0432.CCR-09-3293

had minimal evidence of cortical erosion and mild osteolysis. Quantitative analysis by μCT shows that the tumor-bearing tibias of the bortezomib-treated mice have >2-fold higher bone volume than the tibias of control mice (Fig. 1D). Taken together, these findings show that the bortezomib-treated mice had a striking inhibition of osteolytic disease.

Bortezomib reduces the size of BrCa tumors

The volume of intratibial BrCa tumors was measured *in vivo* in bortezomib- and control-treated mice by injecting the mice with [^{18}F]FDG and visualizing the tumor using PET imaging. Figure 2A shows representative PET images that identify a larger tumor volume and metabolic activity in controls compared with bortezomib-treated mice. A 2-fold increase in tumor volume in the control was confirmed by histologic examination of tibias with tumors from bortezomib and control mice (Fig. 2B and C, left). In controls, there is aggressive lytic disease destroying trabecular and cortical bone with tumor growth invading muscle. In striking contrast, tumor

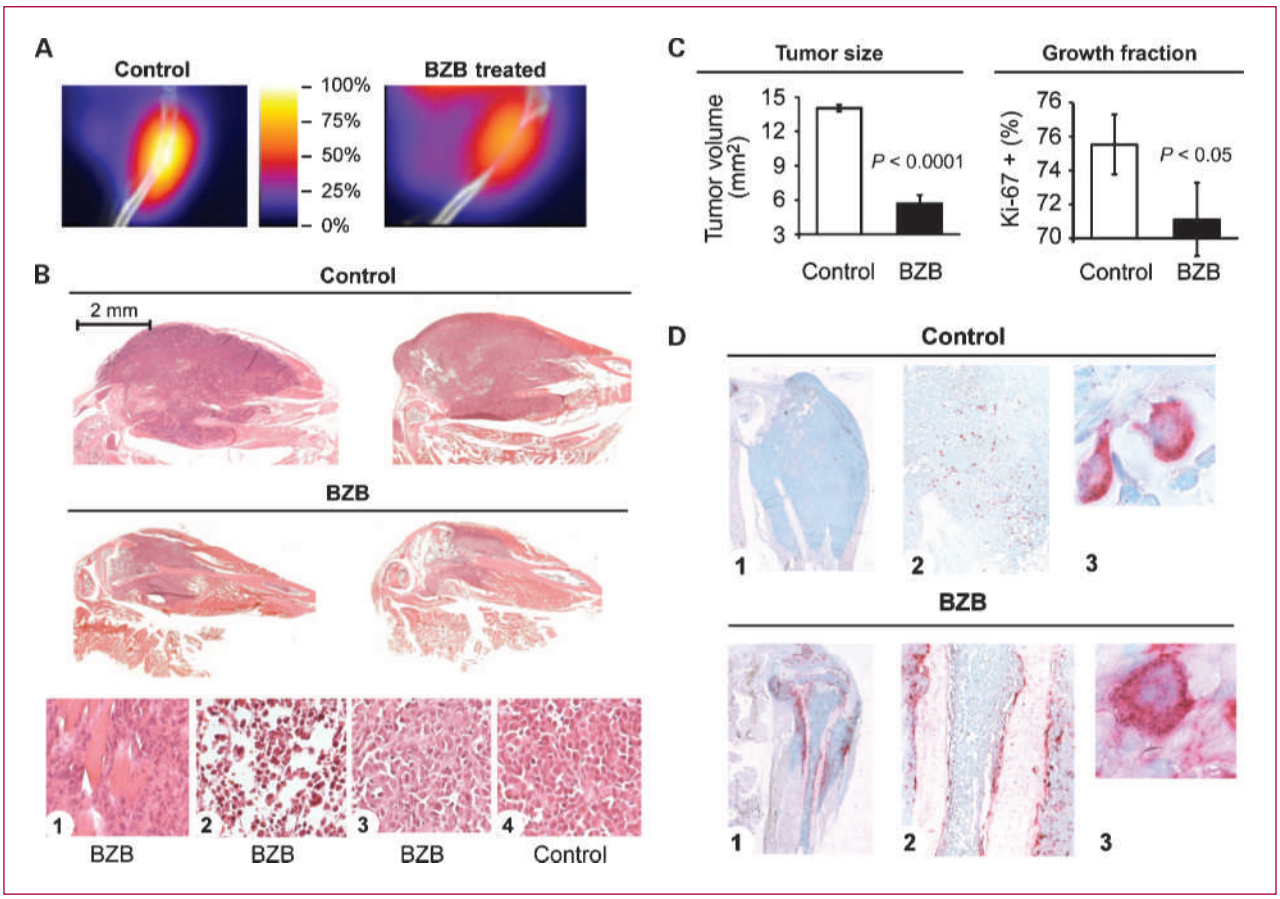

Fig. 2. Bortezomib treatment reduces the size of BrCa tumors implanted in the mouse tibia. A, *in vivo* PET imaging. Thirty-nine days following intratibial injection, mice were injected i.v. with 50 μCi [^{18}F]FDG. Representative PET image reconstructions of the tumor-containing tibial region of bortezomib-treated and control mice overlaid on CT image reconstructions of the same region. The color corresponds to the intensity of the ^{18}F signal and is scaled from bottom to top (black to white) as shown in the color bars, where black indicates 0% radioactivity uptake and white indicates 100% uptake. Higher intensity in the control (white area) reflects the three-dimensional size of the tumor, whereas red areas are those tumor cells with less metabolic activity. Blue is normal tissue cellular activity. Controls exhibited a 50% to 100% (yellow) range of intensity, whereas the bortezomib group showed isotope labeling within the 25% to 50% (orange) intensity range. Standard uptake value for the control mouse is 2.94 g/mL and for the bortezomib-treated mouse is 2.31 g/mL. B, effect of bortezomib on tumor growth and progression (H&E-stained sections). Top, representative histologic sections of proximal tibias from six control and bortezomib-treated mice, showing the tumor size and tibial bone loss. Magnification, ×5. Lower, representative sections of bortezomib- and control-treated tibias. 1, muscle of bortezomib-treated tibia showing tumor growth; 2, marrow cavity of bortezomib-treated tibia with necrotic cells; 3 and 4, area of similar tumor growth in bortezomib (3) and control (4) tibias. Magnification, ×10. C, quantification of tumor size and growth. Left, areas of tumor were selected from multiple histologic sections (n = 5-7) of bortezomib-treated and control tibias (n = 3) and tumor size (mm^2) was calculated. Bortezomib-treated mice had significantly (60%) smaller tumors compared with control mice ($P < 0.0001$). Right, Ki-67 immunohistochemistry was done on bortezomib- and control-treated tumor sections. The Ki-67 growth fraction was calculated as the % of total cells that were positive for Ki-67. The fraction of growing tumor cells was also significantly less in bortezomib tumors than controls (n = 4, $P < 0.05$). D, effect of bortezomib on bone osteolysis as evaluated by TRAP staining. In controls, the cells of the bone surface were already resorbed (panel 1), and only small pieces of fractured bone remained with TRAP-positive cells (panels 2 and 3). In the bortezomib-treated group, bone architecture was preserved (panel 1) and osteoclast activity was present on cortical surfaces (panels 2 and 3). Sections are TRAP stained and presented at ×5 (left), ×10 (middle), and ×40 (right) magnification.

Published OnlineFirst September 15, 2010; DOI: 10.1158/1078-0432.CCR-09-3293

growth in the bortezomib-treated mice was initially restricted to the medullary cavity until a cortical break occurred, allowing slow tumor growth in muscle (Fig. 2B). The bottom panels of Fig. 2B illustrate this point. Viable tumor cells are found in muscle (panel 1) of bortezomib-treated mice, whereas areas of necrotic cells were evident within the medullary cavity (panel 2). Solid tumor tissue outside the bone exhibited similar cell morphology between bortezomib and controls (panels 3 and 4). The fraction of actively growing cells within the tumor was examined by Ki-67 detection and found to be far less in bortezomib-treated tumor than in control tumor (Fig. 2C, right; $P < 0.05$). The modest decrease in tumor growth fraction (% Ki-67$^+$ cells) compared with tumor size can be accounted for by stimulated tumor growth in the bortezomib-treated mice after invasion into muscle.

The effect of tumor growth on bone osteolysis in controls is visualized by minimal detection of osteoclasts by TRAP staining, as there is little bone remaining to be resorbed in controls (Fig. 2D, panel 1). Only small remnants of bone remained with TRAP-positive cells (panels 2 and 3 at ×10 and ×40 magnifications of osteoclasts, respectively). The bortezomib group exhibited osteoclast activity on cortical surfaces, where tumor growth was expanding along the periosteal side as well as on the endosteal surface. These findings suggest that bortezomib treatment reduces osteolytic disease by killing off tumor cells and that remaining tumor cells can still locally secrete osteoclast-activating factors and can survive as a solid tumor.

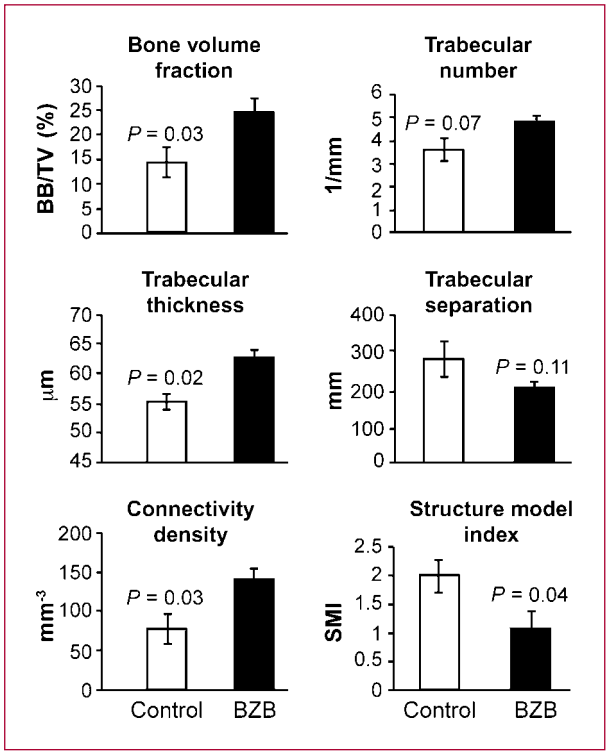

Fig. 3. Bortezomib causes increased bone formation. μCT analysis was done on the distal femurs of NCr/SCID mice 49 d following injection of MDA-MB-231 BrCa cells into the right proximal tibia. Parameters of trabecular bone formation showed significant ($P < 0.05$) increases in bortezomib-treated mice as noted by increased bone volume/total volume, trabecular thickness, and connectivity density. SMI showed a significant ($P < 0.05$) decrease, indicative of a more plate-like architecture in the bortezomib-treated bone.

Bortezomib promotes increased bone formation in the distal femur of the nontumor-bearing limb

BrCa cells secrete many factors that cause local bone resorption and also circulate systemically to affect the entire skeleton. To assess the influence of bortezomib on bone away from the area of the BrCa tumor, μCT analysis was done and various parameters of bone growth were measured in the distal femur of bortezomib-treated and control mice. Figure 3 shows that there is increased trabecular bone formation in femurs of mice treated with bortezomib compared with control as evidenced by significant improvement in the parameters of bone growth, including bone volume fraction, trabecular thickness, connectivity density, and SMI (reflecting a more plate-like architecture in the bortezomib-treated bone). The trabecular number and spacing showed greater bone formation in bortezomib- treated mice, but did not reach significance. These results are entirely consistent with the previously described bone anabolic property of bortezomib (7) and occur in the presence of metastatic tumor growth.

Treatment with bortezomib before tumor cell inoculation protects bone from osteolysis

To assess clinical relevance, a study was designed to establish if bortezomib given before tumor metastasis decreased tumor growth and osteolytic disease and would protect the bone from subsequent osteolysis. Therefore, we examined bortezomib treatment of mice for a period of time before the intratibial inoculation of MDA-MB-231 cells. The rationale was 2-fold. First, the anabolic effect that bortezomib treatment has on bone might render the bone less susceptible to subsequent osteolysis. Second, this has translational relevance, as bortezomib treatment might be used prophylactically to decrease the likelihood of BrCa patients developing osteolytic lesions. The study consisted of three groups: mice that were not treated before or following tumor cell inoculation, mice that were treated with bortezomib (0.3 mg/kg body weight i.p. three times a week) both before and after tumor inoculation, and mice that were treated with bortezomib only before but not after injection of tumor cells (bortezomib pretreatment; Fig. 4A). All three mice in each group exhibited consistent results. Radiographic analysis of the tibias of mice pretreated with bortezomib 3 weeks before time of inoculation with BrCa cells and mice treated continuously with bortezomib both exhibited smaller osteolytic lesions than untreated mice (Fig. 4B). The radiographic grading of the tibias showed a statistically significant lower osteolytic lesion grade in the bortezomib continuous and bortezomib

Published OnlineFirst September 15, 2010; DOI: 10.1158/1078-0432.CCR-09-3293

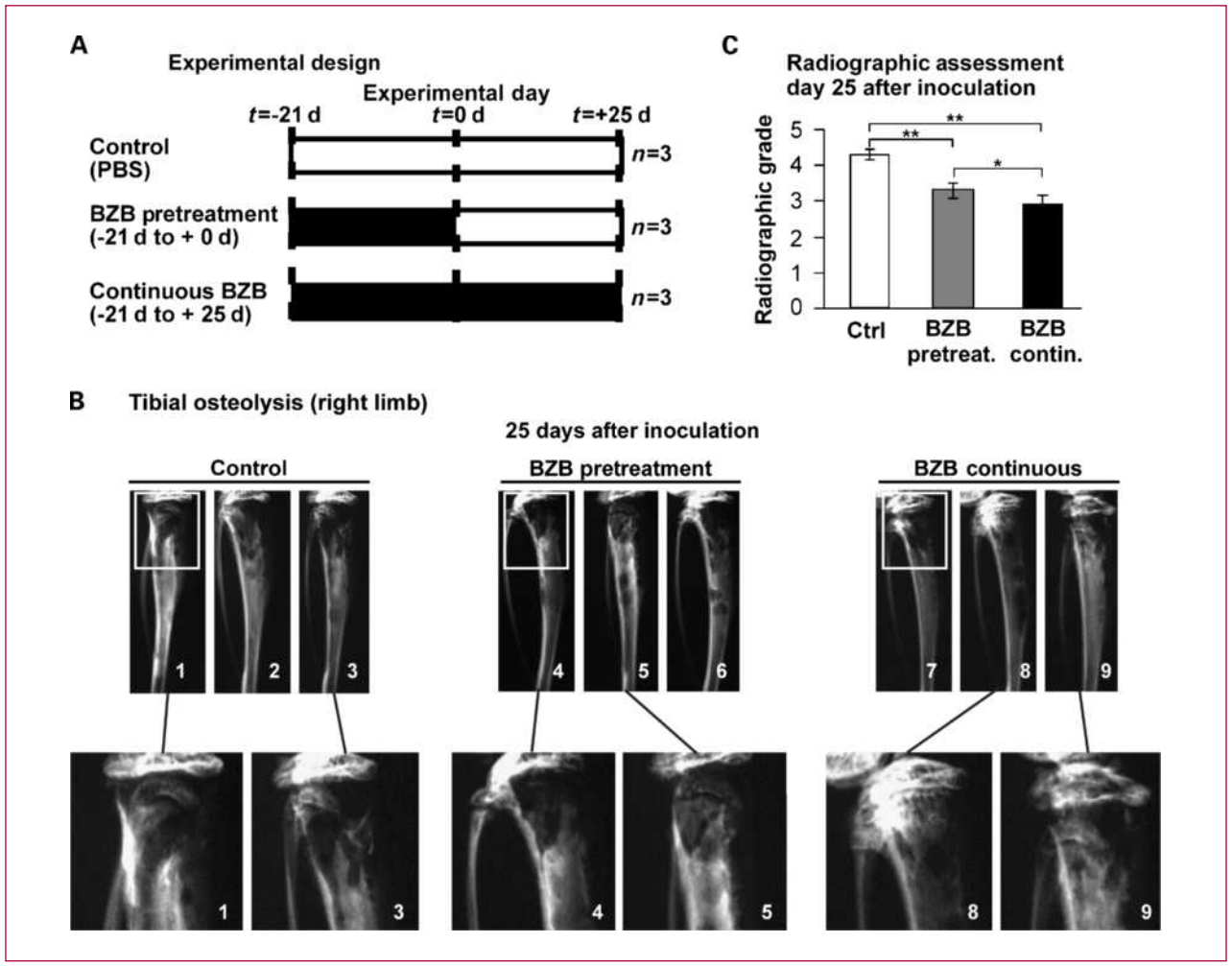

Fig. 4. Treatment with bortezomib before tumor cell inoculation protects bone from osteolysis. A, experimental design. The experiment consisted of three groups: a control group treated with saline from 21 d before intratibial inoculation with BrCa until termination of the experiment at 25 d following inoculation, a bortezomib pretreatment group that received 0.3 mg/kg bortezomib i.p. three times a week for 21 d before BrCa cell inoculation with saline injection for 25 d following inoculation, and a continuous bortezomib treatment group that received 0.3 mg/kg bortezomib i.p. three times a week in both the preinoculation and postinoculation periods. B, radiographic analysis of NCr/SCID mice taken at 25 d following injection of MDA-MB-231 BrCa cells into the right proximal tibia and the treatment conditions described above. Presented are views of the entire tibia ($n = 3$) and representative higher-magnification views of the area in which the majority of the osteolysis occurred. Note the fibular head overlapping the tibia in the area of the osteolytic lesion visualized in lower panel higher magnifications. The tibias of bortezomib pretreated and bortezomib continuous treatment show smaller osteolytic lesions than those in the control group at both time points. C, radiographs were independently scored based on a grading scale developed for osteolytic lesions ($n = 7$ reviewers). Bortezomib pretreatment and bortezomib continuous groups had a lower grade than the control group. Significantly decreased grade was found in bortezomib pretreatment and bortezomib continuous groups compared with control (**, $P < 0.0001$) and bortezomib pretreatment compared with bortezomib continuous group (*, $P < 0.05$).

pretreatment groups compared with control mice with tumors ($P < 0.0001$) and a more effective inhibition of osteolysis in the continuously treated bortezomib group ($P < 0.05$; Fig. 4C).

Patients with metastatic BrCa have a potential for continuously developing new bony lesions. Therefore, we addressed if the anabolic effect of bortezomib treatment on bones that did not contain tumor (shown in Fig. 3) would provide protection to the skeleton in a patient with advanced BrCa, and if this effect would remain over time despite the presence of tumor at a remote site. To determine if treatment with bortezomib may protect the skeleton from subsequent osteolysis, μCT analysis of the femurs of the three groups of mice described above (Fig. 4A) was done examining both femurs of each group. Several significant changes are observed in trabecular bone structure between the control and the two bortezomib groups and between the left femur and the right femur (Fig. 5). Bortezomib treatment supports increased trabecular bone formation in both tumor-bearing (right) and contralateral (left) limbs reflected in all parameters of trabecular bone, in both bortezomib continuous and pretreatment groups, compared with control (Fig. 5, continuous versus control; $P < 0.05$ to $P < 0.005$). Both

Published OnlineFirst September 15, 2010; DOI: 10.1158/1078-0432.CCR-09-3293

pretreatment and continuous bortezomib groups exhibited a significant improvement in bone formation (~60% increase in bone volume) compared with control. However, it is noteworthy that the femurs from the tumor-affected right leg of both bortezomib and control mice consistently have values that indicate less bone when compared with the left femurs (Fig. 5, right versus left). This suggests that mice develop disuse osteopenia in the right femur as a result of decreased weight bearing on the tumored leg. The bone anabolic effects of bortezomib were not attenuated during the subsequent tumor growth period. Mice receiving a 21-day course of bortezomib before treatment (before inoculation of tumor cells) did not have significantly different bone parameters compared with the mice receiving continuous treatment (Fig. 5, continuous versus pretreatment; $P > 0.05$). This effect is significant in that a pulsed dose of bortezomib before inoculation of cancer cells was sufficient to confer an anabolic effect on bone and provide protection from osteolysis. We conclude, from the increased bone volume following 3 weeks of pretreatment in the nontumored femur and the reduced tibial osteolysis after inoculation during the following 25 days of tumor growth, that bortezomib could contribute to protecting the skeleton in advanced BrCa.

Bortezomib decreases survival of MDA-MB-231 BrCa cells and affects gene expression

To gain insight into the mechanisms of bortezomib on the cellular activities of BrCa cells, cell growth and mRNA levels of metastatic and osteolytic genes were examined. MDA-MB-231 proliferating cells were treated *in vitro* with varying doses of bortezomib, ranging from 0 to 50 nmol/L, to determine the effects on cell proliferation and survival. Initial cell count studies done after 24 hours showed that adherent cell counts decreased beginning at 10 nmol/L bortezomib (21% of control), with a 62% and 74% cell loss at 20 and 50 nmol/L bortezomib, respectively (data not shown). The loss of cell viability by bortezomib was the result mainly of necrosis of the cells as determined by an Annexin V binding assay done on proliferating cells treated with varying doses of bortezomib (Fig. 6A). FACS analysis of the cells (represented in Fig. 6B) showed that the percentage of viable cells (neither stained with PI nor bound to Annexin V; Fig. 6A, solid line, diamond; Fig. 6B, bottom-left quadrant) decreased steadily to 60% at a dose of 20 nmol/L bortezomib and then remained constant to a dose of 50 nmol/L bortezomib. The percentage of cells undergoing apoptosis (bound to Annexin V, but not stained with PI; Fig. 6A, dashed line, open square; Fig. 6B, bottom-right quadrant) did not exceed 10%. The amount of cells undergoing necrosis (bound to Annexin V and stained with PI; Fig. 6A, solid line, circle; Fig. 6B, upper-right quadrant) was greater than that of apoptotic cells and remained relatively constant from bortezomib doses of 10 to 50 nmol/L. These results indicate that both necrosis and apoptosis contribute to death of MDA-MB-231 cells by bortezomib treatment, but also suggest that the MDA-MB-231 cell line may have a small population of bortezomib-resistant cells.

We determined the contribution of bortezomib in preventing osteolytic disease by analyzing dose-dependent expression of marker genes associated with bone resorption and formation in MDA-MB-231 cells treated 24 hours with bortezomib (Fig. 6C). Expression of genes promoting tumor growth (*RUNX2*, *MMP-9*, and *VEGF*) decreased at increased bortezomib concentrations, whereas GAPDH, an internal marker of cellular RNA

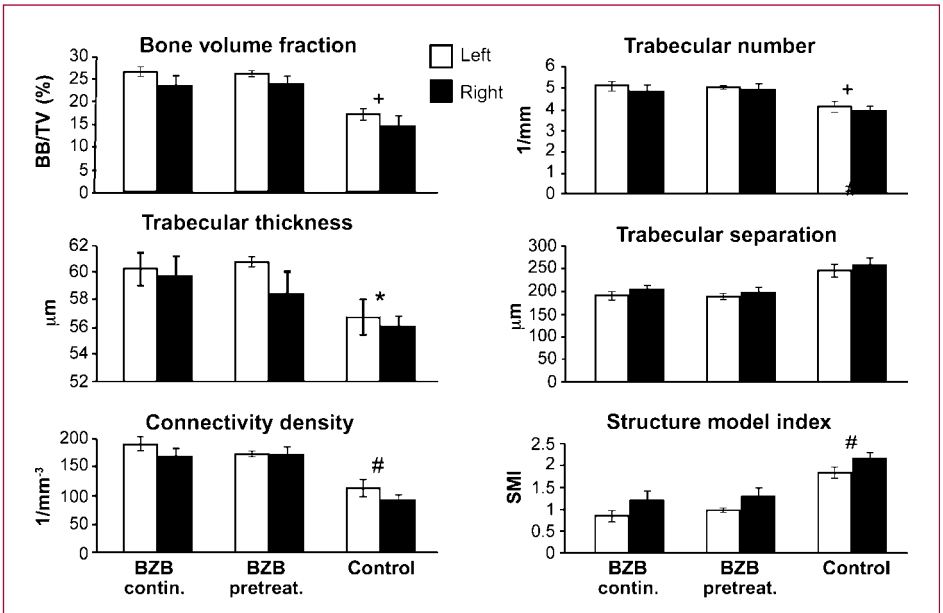

Fig. 5. Anabolic effects of bortezomib in tumor-bearing and contralateral femurs. µCT analysis was done on the bilateral distal femurs of the mice from the three treatment groups described in Fig. 4 ($n = 3$). In all measured parameters, there is a significant anabolic effect evident in both bortezomib pretreatment and continuous treatment groups compared with controls. Note that the right femur, proximal to the tumor-bearing tibia, has less bone than the contralateral femur. *, $P < 0.05$; +, $P < 0.001$; #, $P < 0.0005$.

Published OnlineFirst September 15, 2010; DOI: 10.1158/1078-0432.CCR-09-3293

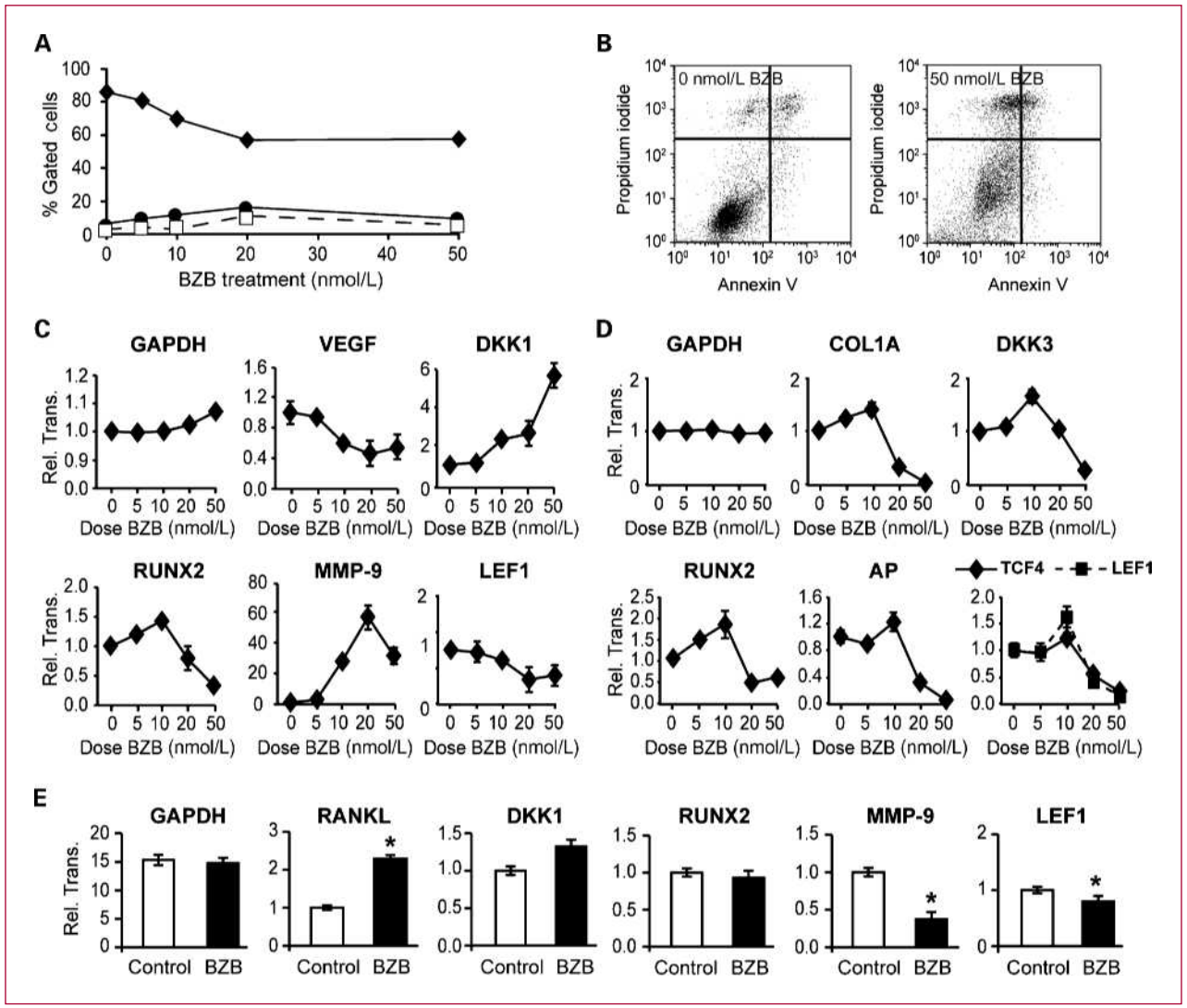

Fig. 6. Bortezomib treatment reduces cell proliferation and decreases cell viability of BrCa cells *in vitro* but does not induce significant apoptosis. A, the relative number of viable cells, necrotic cells, and cells undergoing apoptosis following treatment with bortezomib in the range of 0 to 50 nmol/L for 14 h was measured by binding of FITC-conjugated Annexin V and staining with PI followed by FACS analysis. The percentage of gated cells that were Annexin V and PI negative (live cell, solid line, diamond), Annexin V positive and PI negative (apoptotic cells, dashed line, open square), and Annexin V and PI positive (necrotic cells, solid line, circle) are shown as a function of the increasing concentration of bortezomib treatment. B, bivariate plots of the primary FACS data for ungated cells treated with 0 and 50 nmol/L bortezomib. The quadrants, which are defined using FACSCalibur software and represent cells that are Annexin V and PI negative (bottom left), Annexin V positive and PI negative (bottom right), Annexin V negative and PI positive (top left), and Annexin V and PI positive (top right), show a far greater proportion of cells in the quadrant representing necrosis in response to bortezomib treatment. C, the amount of transcript of various genes in MDA-MB-231 cells treated with bortezomib in the range of 0 to 50 nmol/L bortezomib for 24 h was measured using quantitative PCR and standardized to the amount of GAPDH transcript in the same cells. The amount of transcript relative to no bortezomib treatment is shown for each concentration of bortezomib treatment used. The CT values for monitored genes were between 18 and 25, except for MMP-9 (CT, 35). D, gene transcript levels were measured in MC3T3 osteoblast-like cells following 24-h treatment with 0 to 50 nmol/L bortezomib using quantitative PCR, as described above. The CT values were all <21. E, tumor tissue from mice treated with bortezomib or control for 28 d was analyzed for relevant gene expression by quantitative PCR. The amount of transcript of bortezomib-treated tumors relative to control is shown. The CT values were between 16 and 35 for all the monitored genes (all <30, except RANKL). Significant differences were seen in RANKL, MMP-9, and LEF1 ($P < 0.05$, $n = 5$).

levels, remained constant. In response to bortezomib, we found a steady increase in expression of the Wnt antagonist DKK1 (31), with a concomitant decrease in the canonical Wnt transcription factor LEF1. This finding indicated that bortezomib is inhibiting tumor cell growth mediated by the Wnt pathway, as well as reducing the levels of genes in MDA-MB-231 cells related to osteolytic activity in bone (32).

To evaluate the mechanism for the anabolic effect of bortezomib on bone formation, we examined a preosteoblast cell line (MC3T3) analogous to osteoprogenitor cells within the marrow for its responsiveness to the same dose

Published OnlineFirst September 15, 2010; DOI: 10.1158/1078-0432.CCR-09-3293

range that affects BrCa cells (Fig. 6D). The high doses of 20 and 50 nmol/L were toxic to both cell types, osteoblasts and BrCa cells, resulting in loss of expression of bone formation markers (*COL1* and *AP* in the osteoblasts). A striking difference between BrCa and MC3T3 cells was the opposite effects on the Wnt pathway, which was inhibited in the tumor cells but was stimulated in osteoblasts at lower doses for bone formation. This finding is consistent with the anabolic effect of bortezomib in multiple myeloma (33). We next determined if the same effects occurred in response to the *in vivo* dose of bortezomib. Tumor tissue excised from the tibia showed a striking inhibition of MMP-9 with a modest increase in DKK, consistent with the *in vitro* effect of bortezomib in BrCa cells. Additionally, in the tumor tissue, RANKL, promoting bone resorption, was stimulated. This finding reflects the histologic analyses of the bortezomib-treated group (see Fig. 2D) exhibiting osteoclastic activity.

We conclude from these studies that metastasis-associated osteolytic disease is reduced *in vivo* by bortezomib through multiple mechanisms in the bone microenvironment: by inducing cellular necrosis, decreasing the tumor response to Wnt signaling, reducing expression of a key factor in tumor vascularization, and decreasing the RUNX2 and MMP-9 osteolytic cascade. Together, these modifications in tumor cell activity by bortezomib contribute to inhibiting tumor growth to the bone microenvironment.

Discussion

Here, we established that the proteasome inhibitor bortezomib effectively suppresses BrCa tumor growth within bone and stimulates new bone formation in the presence of metastatic disease. Antitumor growth effects by bortezomib occur in the bone microenvironment, where the vicious cycle of tumor growth and osteolytic disease is activated in response to BrCa cells. We show that the anti-osteolytic effects of bortezomib are primarily due to significantly decreased tumor size as evidenced by histology, radiographic monitoring, and μCT quantitation of bone volume. Lastly, we have defined mechanisms contributing to the inhibition of tumor growth in the bone microenvironment and osteolytic disease by bortezomib that include (*a*) the sensitivity of highly metastatic BrCa cells to necrosis, (*b*) reduction in expression of metastatic and tumor growth–related genes, and (*c*) promotion of bone formation throughout the skeleton. These effects of bortezomib provide a beneficial antitumor and bone anabolic effect.

In our continuously treated study, we find a striking inhibition of osteolytic disease that continued through 4 weeks after inoculation. However, at 5 weeks, evidence of the onset of osteolysis was identified in the bortezomib group, which slowly progressed until the study was terminated when tumor size became unbearable in the control group (7 or 8 weeks in repeat study). The Ki-67 assays suggest that surviving tumor cells exposed to bortezomib result in a delayed onset of osteolysis. As our bortezomib dose did not cause toxic effects in mice, perhaps a higher dose would be more effective in killing all BrCa cells, as indicated from our *in vitro* studies. Two mechanisms are contributing to reduced osteolytic disease: the killing of tumor cells by bortezomib and bortezomib inhibition of osteoclast activity through induction of apoptosis, which has been identified in several studies (17–19, 23–26). BrCa cells are known to produce many different factors that induce osteolytic disease. Notably, at sacrifice after 7 weeks, we observe TRAP-positive osteoclasts at the tumor-bone interface in bortezomib-treated mice and also found RANKL to be expressed in the tumor tissue. Our *in vitro* studies analyzing bortezomib dose effects suggest that a small population of MDA-MB-231 cells survive at high doses.

Early studies found mixed results in ongoing clinical trials evaluating the effect of bortezomib on osteolytic lesions caused by solid tumors (34–37). However, in one other study using the intratibial model of prostate cancer, it was suggested that osteoclast activity was diminished (38), similar to what has been shown in multiple myeloma patients (39). In our studies, the net effect of systemic bortezomib is that proteasome inhibition is effective in preventing BrCa tumor growth in bone and greatly diminishes the osteolytic disease. Thus, just as bortezomib is used for multiple myeloma cells that have increased proteasome activity (40) inducing osteolytic bone disease [as does BrCa (18)], we find that bortezomib has the similar anti-osteolytic effects in BrCa tumors.

We identified mechanisms that are directly attributed to bortezomib, modifying the properties of BrCa cells *in vivo* to facilitate an anabolic effect in the bone microenvironment in the presence of a tumor. Analysis of the tumor tissue revealed a reduction in the metastasis-related genes RUNX2, VEGF, and MMP-9 at high doses of bortezomib. This profile reflects altered cellular properties, reduced tumor vascularization, migration, matrix destruction, and osteolytic disease (27, 30, 41–44). Another mechanism of bortezomib inhibiting tumor growth is by elevation of DKK1, an inhibitor of the Wnt signaling pathway, and a concomitant decrease in LEF1, the transcriptional mediator of Wnt signaling, thereby decreasing tumor growth potential. In multiple myeloma patients, serum levels of DKK are very low, contributing to activated Wnt signaling (21, 22). BrCa tumorigenesis and bone metastasis are linked to the Wnt signaling pathway, having downregulated DKK and dysregulation of β-catenin linked to progression and prognosis (31, 45–47). These beneficial effects of bortezomib are also observed in the tumor tissue by the changes in expressed genes (reduced LEF1 and MMP-9). Notably, osteoblasts have the opposite response at low bortezomib doses, exhibiting increased LEF1/TCF4, AP, and COL1 and reflecting bone formation activity. In multiple myeloma patients, bortezomib stimulates osteoblast activity (22, 33), consistent with the significant anabolic effect of bortezomib in the nontumor-bearing limbs of mice with bone tumors.

Published OnlineFirst September 15, 2010; DOI: 10.1158/1078-0432.CCR-09-3293

Our studies are significant, as the anabolic effects of bortezomib on BrCa-free bone in the setting of metastatic bone disease were shown by a 1.5-fold increase in bone volume. Furthermore, we showed that the effects of a 3-week pretreatment allowed accrual of bone throughout the skeleton from the analyses of the nontumor-bearing femurs. This suggests a preemptive, protective effect to the bone, thereby diminishing the effect of tumor-mediated osteolysis. Thus, we find an additional benefit to the anabolic bone effect, as pretreatment with bortezomib has a repressive effect on subsequent tumor growth. The clinical implications of these results are considerable. Proteasome inhibitors could provide a protective effect on the skeleton if bortezomib were to be combined with other treatments for BrCa before metastasis.

In summary, proteasome inhibitors may treat solid tumors and the osteolytic bone disease that accompanies metastasis by myriad effects that include decreasing tumor cell proliferation and survival, inhibiting bone-destructive pathways and enzymes and vascularity of the tumors, reducing osteoclast number and function (17, 24, 25, 39), and increasing osteoblast differentiation and bone formation (7, 9, 22, 33). Our studies show inhibitory effects of bortezomib on solid tumor (BrCa) growth in bone and prevention of the early-onset osteolytic disease. We conclude that proteasome inhibitors have multifactorial beneficial effects in prevention of BrCa growth in bone and induced osteolysis.

Disclosure of Potential Conflicts of Interest

D.C. Ayers: commercial research grant, Zimmer, Inc.; other commercial research support, Musculoskeletal Transplant Foundation (MTF).

Grant Support

Studies reported were in part supported by NIH grants P01CA082834, S10RR023540, and F32AR055030. Core resources supported by the Diabetes Endocrinology Research Center grant DK32520 were also used. J.B. Lian is a member of the University of Massachusetts Diabetes and Endocrinology Resource Center (DK32520). The contents of this manuscript are solely the responsibility of the authors and do not necessarily represent the official views of the NIH.

The costs of publication of this article were defrayed in part by the payment of page charges. This article must therefore be hereby marked *advertisement* in accordance with 18 U.S.C. Section 1734 solely to indicate this fact.

Received 12/15/2009; revised 08/19/2010; accepted 08/25/2010; published OnlineFirst 09/15/2010.

References

1. Spataro V, Norbury C, Harris AL. The ubiquitin-proteasome pathway in cancer. Br J Cancer 1998;77:448–55.
2. Adams J, Palombella VJ, Sausville EA, et al. Proteasome inhibitors: a novel class of potent and effective antitumor agents. Cancer Res 1999;59:2615–22.
3. Ande SR, Chen J, Maddika S. The ubiquitin pathway: an emerging drug target in cancer therapy. Eur J Pharmacol 2009;625:199–205.
4. Giuliani N, Morandi F, Tagliaferri S, et al. The proteasome inhibitor bortezomib affects osteoblast differentiation *in vitro* and *in vivo* in multiple myeloma patients. Blood 2007;110:334–8.
5. Heider U, Kaiser M, Muller C, et al. Bortezomib increases osteoblast activity in myeloma patients irrespective of response to treatment. Eur J Haematol 2006;77:233–8.
6. Zangari M, Esseltine D, Lee CK, et al. Response to bortezomib is associated to osteoblastic activation in patients with multiple myeloma. Br J Haematol 2005;131:71–3.
7. Mukherjee S, Raje N, Schoonmaker JA, et al. Pharmacologic targeting of a stem/progenitor population *in vivo* is associated with enhanced bone regeneration in mice. J Clin Invest 2008;118:491–504.
8. Qiang YW, Hu B, Chen Y, et al. Bortezomib induces osteoblast differentiation via Wnt-independent activation of β-catenin/TCF signaling. Blood 2009;113:4319–30.
9. Pennisi A, Li X, Ling W, Khan S, Zangari M, Yaccoby S. The proteasome inhibitor, bortezomib suppresses primary myeloma and stimulates bone formation in myelomatous and nonmyelomatous bones *in vivo*. Am J Hematol 2009;84:6–14.
10. Shimazaki C, Uchida R, Nakano S, et al. High serum bone-specific alkaline phosphatase level after bortezomib-combined therapy in refractory multiple myeloma: possible role of bortezomib on osteoblast differentiation. Leukemia 2005;19:1102–3.
11. Terpos E, Sezer O, Croucher P, Dimopoulos MA. Myeloma bone disease and proteasome inhibition therapies. Blood 2007;110:1098–104.
12. Gnant M, Mlineritsch B, Schippinger W, et al. Endocrine therapy plus zoledronic acid in premenopausal breast cancer. N Engl J Med 2009;360:679–91. Erratum in: N Engl J Med 2009;360:2379.
13. Valachis A, Polyzos NP, Georgoulias V, Mavroudis D, Mauri D. Lack of evidence for fracture prevention in early breast cancer bisphosphonate trials: a meta-analysis. Gynecol Oncol 2010;117:139–45.
14. Costa L. Bisphosphonates: reducing the risk of skeletal complications from bone metastasis. Breast 2007;16 Suppl 3:S16–20.
15. Diel IJ, Bergner R, Grotz KA. Adverse effects of bisphosphonates: current issues. J Support Oncol 2007;5:475–82.
16. King AE, Umland EM. Osteonecrosis of the jaw in patients receiving intravenous or oral bisphosphonates. Pharmacotherapy 2008;28:667–77.
17. von Metzler I, Krebbel H, Hecht M, et al. Bortezomib inhibits human osteoclastogenesis. Leukemia 2007;21:2025–34.
18. Roodman GD. Pathogenesis of myeloma bone disease. Leukemia 2009;23:435–41.
19. Uy GL, Trivedi R, Peles S, et al. Bortezomib inhibits osteoclast activity in patients with multiple myeloma. Clin Lymphoma Myeloma 2007;7:587–9.
20. Garrett IR, Chen D, Gutierrez G, et al. Selective inhibitors of the osteoblast proteasome stimulate bone formation *in vivo* and *in vitro*. J Clin Invest 2003;111:1771–82.
21. Terpos E, Heath DJ, Rahemtulla A, et al. Bortezomib reduces serum dickkopf-1 and receptor activator of nuclear factor-κB ligand concentrations and normalises indices of bone remodelling in patients with relapsed multiple myeloma. Br J Haematol 2006;135:688–92.
22. Heider U, Kaiser M, Mieth M, et al. Serum concentrations of DKK-1 decrease in patients with multiple myeloma responding to anti-myeloma treatment. Eur J Haematol 2009;82:31–8.
23. Ahn KS, Sethi G, Chao TH, et al. Salinosporamide A (NPI-0052) potentiates apoptosis, suppresses osteoclastogenesis, and inhibits invasion through down-modulation of NF-κB regulated gene products. Blood 2007;110:2286–95.
24. Zavrski I, Krebbel H, Wildemann B, et al. Proteasome inhibitors abrogate osteoclast differentiation and osteoclast function. Biochem Biophys Res Commun 2005;333:200–5.
25. Hongming H, Jian H. Bortezomib inhibits maturation and function of osteoclasts from PBMCs of patients with multiple myeloma by downregulating TRAF6. Leuk Res 2009;33:115–22.
26. Boissy P, Andersen TL, Lund T, Kupisiewicz K, Plesner T, Delaisse JM. Pulse treatment with the proteasome inhibitor bortezomib inhibits

Published OnlineFirst September 15, 2010; DOI: 10.1158/1078-0432.CCR-09-3293

osteoclast resorptive activity in clinically relevant conditions. Leuk Res 2008;32:1661–8.
27. Pratap J, Wixted JJ, Gaur T, et al. Runx2 transcriptional activation of Indian hedgehog and a downstream bone metastatic pathway in breast cancer cells. Cancer Res 2008;68:7795–802.
28. Bouxsein ML, Myers KS, Shultz KL, Donahue LR, Rosen CJ, Beamer WG. Ovariectomy-induced bone loss varies among inbred strains of mice. J Bone Miner Res 2005;20:1085–92.
29. Glatt V, Canalis E, Stadmeyer L, Bouxsein ML. Age-related changes in trabecular architecture differ in female and male C57BL/6J mice. J Bone Miner Res 2007;22:1197–207.
30. Rajagopalan S, Lu L, Yaszemski MJ, Robb RA. Optimal segmentation of microcomputed tomographic images of porous tissue-engineering scaffolds. J Biomed Mater Res A 2005;75:877–87.
31. Zhou XL, Qin XR, Zhang XD, Ye LH. Downregulation of Dickkopf-1 is responsible for high proliferation of breast cancer cells via losing control of Wnt/β-catenin signaling. Acta Pharmacol Sin 2010;31: 202–10.
32. Pratap J, Lian JB, Stein GS. Metastatic bone disease: role of transcription factors and future targets. Bone 2010 [Epub ahead of print].
33. Oyajobi BO, Garrett IR, Gupta A, et al. Stimulation of new bone formation by the proteasome inhibitor, bortezomib: implications for myeloma bone disease. Br J Haematol 2007;139:434–8.
34. Cresta S, Sessa C, Catapano CV, et al. Phase I study of bortezomib with weekly paclitaxel in patients with advanced solid tumours. Eur J Cancer 2008;44:1829–34.
35. Schmid P, Kuhnhardt D, Kiewe P, et al. A phase I/II study of bortezomib and capecitabine in patients with metastatic breast cancer previously treated with taxanes and/or anthracyclines. Ann Oncol 2008;19:871–6.
36. Engel RH, Brown JA, Von Roenn JH, et al. A phase II study of single agent bortezomib in patients with metastatic breast cancer: a single institution experience. Cancer Invest 2007;25:733–7.
37. Yang CH, Gonzalez-Angulo AM, Reuben JM, et al. Bortezomib (VELCADE) in metastatic breast cancer: pharmacodynamics, biological effects, and prediction of clinical benefits. Ann Oncol 2006;17:813–7.
38. Whang PG, Gamradt SC, Gates JJ, Lieberman JR. Effects of the proteasome inhibitor bortezomib on osteolytic human prostate cancer cell metastases. Prostate Cancer Prostatic Dis 2005;8:327–34.
39. Terpos E. Bortezomib directly inhibits osteoclast function in multiple myeloma: implications into the management of myeloma bone disease. Leuk Res 2008;32:1646–7.
40. Edwards CM, Lwin ST, Fowler JA, et al. Myeloma cells exhibit an increase in proteasome activity and an enhanced response to proteasome inhibition in the bone marrow microenvironment *in vivo*. Am J Hematol 2009;84:268–72.
41. Pratap J, Javed A, Languino LR, et al. The Runx2 osteogenic transcription factor regulates matrix metalloproteinase 9 in bone metastatic cancer cells and controls cell invasion. Mol Cell Biol 2005; 25:8581–91.
42. Pratap J, Imbalzano K, Underwood J, et al. Ectopic Runx2 expression in mammary epithelial cells disrupts formation of normal acini structure: implications for breast cancer progression. Cancer Res 2009;69:6807–14.
43. Greenberg JI, Cheresh DA. VEGF as an inhibitor of tumor vessel maturation: implications for cancer therapy. Expert Opin Biol Ther 2009; 9:1347–56.
44. Roland CL, Dineen SP, Lynn KD, et al. Inhibition of vascular endothelial growth factor reduces angiogenesis and modulates immune cell infiltration of orthotopic breast cancer xenografts. Mol Cancer Ther 2009;8:1761–71.
45. Lopez-Knowles E, Zardawi SJ, McNeil CM, et al. Cytoplasmic localization of β-catenin is a marker of poor outcome in breast cancer patients. Cancer Epidemiol Biomarkers Prev 2010;19:301–9.
46. Previdi S, Maroni P, Matteucci E, Broggini M, Bendinelli P, Desiderio MA. Interaction between human-breast cancer metastasis and bone microenvironment through activated hepatocyte growth factor/Met and β-catenin/Wnt pathways. Eur J Cancer 2010;46:1679–91.
47. Barnes GL, Javed A, Waller SM, et al. Osteoblast-related transcription factors Runx2 (Cbfa1/AML3) and MSX2 mediate the expression of bone sialoprotein in human metastatic breast cancer cells. Cancer Res 2003;63:2631–7.